



Using a zero-magnetization ferromagnet as the pinning layer in exchange-bias systems

M. Ungureanu,¹ K. Dumesnil,¹ C. Dufour,¹ N. Gonzalez,¹ F. Wilhelm,² A. Smekhova,² and A. Rogalev²

¹*Institut Jean Lamour (UMR CNRS 7198), Université Henri Poincaré Nancy, BP 239, 54506 Vandoeuvre les Nancy Cedex, France*

²*European Synchrotron Radiation Facility, 6 rue Jules Horowitz, BP 220, 38043 Grenoble, France*

(Received 16 July 2010; revised manuscript received 13 September 2010; published 15 November 2010)

Exchange bias properties have been investigated in a ($\text{Sm}_{1-x}\text{Gd}_x\text{Al}_2/\text{SmAl}_2$) bilayer (for $x=0.028$) with perpendicular magnetization, an original exchange-coupled system based on the zero magnetization ferromagnet ($\text{Sm}_{1-x}\text{Gd}_x\text{Al}_2$) as the pinning layer. This unusual magnet exhibits a magnetic compensation temperature where it presents both a zero magnetization and a long-range spin ferromagnetic order. In the ($\text{Sm}_{1-0.028}\text{Gd}_{0.028}\text{Al}_2/\text{SmAl}_2$) bilayer, a large positive exchange bias has been observed for the SmAl_2 magnetization reversal, attesting for the exchange coupling between both compounds, even at the $\text{Sm}_{1-0.028}\text{Gd}_{0.028}\text{Al}_2$ magnetic compensation temperature; the magnetization of the $\text{Sm}_{1-0.028}\text{Gd}_{0.028}\text{Al}_2$ part of the bilayer appears to be pinned but the pinned component is obviously smaller than the one observed in a single uncovered $\text{Sm}_{1-0.028}\text{Gd}_{0.028}\text{Al}_2$. X-ray Magnetic Circular Dichroism experiments have been undertaken to investigate the magnetization reversal in both layers independently and more particularly to probe the $\text{Sm}_{1-0.028}\text{Gd}_{0.028}\text{Al}_2$ behavior in its zero-magnetization state. They reveal that approximately 20% of the $\text{Sm}_{1-0.028}\text{Gd}_{0.028}\text{Al}_2$ layer is driven to reverse by exchange coupling to SmAl_2 . The presence of lateral domains in the $\text{Sm}_{1-0.028}\text{Gd}_{0.028}\text{Al}_2$ layer likely accounts for the relatively large proportion of rotatable moments and for the observed temperature dependence of exchange-bias field.

DOI: [10.1103/PhysRevB.82.174421](https://doi.org/10.1103/PhysRevB.82.174421)

PACS number(s): 75.70.Cn, 75.90.+w, 75.30.Et

I. INTRODUCTION

Exchange-coupled systems refer to heterostructures combining different magnetic materials that are coupled by exchange interactions in the regions where they are in contact. Such heterostructures can be magnetic clusters embedded in a magnetic matrix, multilayers, and superlattices, or more simply a bilayer system. Exchange-coupled systems are of particular interest because they permit designing specific materials with tailored magnetic properties, such as coercivity,¹ magnetization reversal process,² etc. Exchange coupling may also give rise to the so-called “exchange bias” (EB),^{3,4} a phenomenon characterized by the horizontal shift of the magnetic hysteresis loops. It is now commonly used in magnetic devices, especially in “spin valves,” to pin the magnetization of a ferromagnetic layer in a given direction.⁵ The large majority of systems that have been investigated for their exchange-bias properties are those combining antiferromagnetic (AFM) and ferromagnetic (FM) materials, in which EB appears when the sample is cooled down in an applied magnetic field from a temperature higher than the ordering temperature of the AFM. Beyond those AFM/FM systems, exchange bias has been also reported in systems combining ferrimagnetic materials,^{6–8} more generally, in systems combining hard and soft magnetic materials (HM/SM),⁹ and even in a single magnetic compound system.^{10,11} Despite the large amount of research works devoted to this topic, EB is not fully understood. Several mechanisms are suggested to account for experimental observations^{12,13} but one of the difficulties in describing EB effects with accuracy relies on the combination of different phenomena in real systems. Most theories of exchange bias however require *pinned moments* that resist to the external field and *uncompensated moments* in this pinned component that enable the coupling to the unpinned part. In conventional AFM/FM systems, AFM

moments are naturally pinned because of the zero net magnetization but the zero magnetization makes the study of this AFM pinned layer difficult. Uncompensated magnetization is challenging to detect and quantify and highly sensitive specific experimental techniques such as x-ray magnetic circular dichroism (XMCD)^{14–16} and polarized neutron reflectometry^{17–19} are generally required. In HM/SM systems, the hard material can play the role of the pinning layer, provided that the external field does not overcome its coercive field.^{6,7} Uncompensated magnetization is then much larger and yields stronger exchange-bias fields than in usual AFM/FM. Such systems attract lots of interest because they permit an easier analysis of the pinning part. In contrast to AFM this pinning part however still exhibits a net magnetization that can interact with the external field and give rise for example to demagnetizing field effects.

The study presented in this paper deals with an original exchange-coupled system in which the pinning layer is a new kind of magnetic material: a zero-magnetization ferromagnet (ZMF). As an AFM material, the ZMF does not interact with any external magnetic field. However, due to its ferromagnetic spin order, it can still strongly couple to a FM material and it can be easily investigated by electronic selective techniques such as XMCD. The first experimental realization of a ZMF was achieved by Adachi *et al.*²⁰ whose main objective was to obtain a material that would be able to spin polarize an electric current without exhibiting any magnetization. Such an unusual magnet would be of particular interest in devices dealing with the spin of electrons. These authors have synthesized the first ZMF by substituting a small amount of Sm atoms by Gd ones in the SmAl_2 intermetallic compound. SmAl_2 (SA) is a ferromagnet with a small magnetization, resulting from antiparallel spin (S) and orbital (L) contributions, and dominated by L moments over the entire temperature range.²¹ In $\text{Sm}_{1-x}\text{Gd}_x\text{Al}_2$ (SGA), the supplement-

tal pure spin contribution from Gd atoms leads to a magnetic compensation point ($M=0$) at the so-called compensation temperature (T_{comp}), where S and L contributions perfectly cancel each other. L moments are the dominant contribution to magnetization below T_{comp} , and S moments are dominant above T_{comp} .²² The nature of this unusual compensated state results in the persisting long-range ferromagnetic order of S moments.^{23,24}

Our group has proved the possibility to grow this material as epitaxial films of high crystal quality.²⁵ We have shown that epitaxial films still gather interesting properties required for fundamental studies in the field of spin-resolved devices: they do exhibit a magnetic compensated state that is directly related to the Gd content²⁶ and this compensated state coexists with a long-range ferromagnetic order.²⁷

The spin ferromagnetic order is expected to enable the coupling of the SGA layer to a FM layer, even in the SGA compensated state. This opens the way of interesting analysis of unusual ZMF/FM exchange-bias systems in comparison with conventional AFM/FM. Moreover, as it will be presented in the following, the remaining ferromagnetic spin order enables the investigation of the zero-magnetization pinning layer, in particular, by XMCD.

In this paper we report on the magnetic behavior in a specific $\text{Sm}_{1-x}\text{Gd}_x\text{Al}_2/\text{SmAl}_2$ bilayer (for $x=0.028$). This system combines a ferromagnetic material (SA) dominated by the Sm orbital contribution over the entire temperature range, and the unusual ferromagnet (SGA), the magnetization of which drops to zero at T_{comp} and is dominated by either the orbital or spin contribution, respectively, below and above T_{comp} . This study aims first at investigating exchange-bias properties in this bilayer and more particularly to analyze how the SA magnetization reversal affects the SGA moments, especially in the magnetic compensated state. This has been achieved in combining classical magnetometry [superconducting quantum interference device (SQUID)] with XMCD measurements performed at both Sm and Gd absorption edges. The paper is structured as follows: Sec. II contains details about the sample growth and investigating methods; SQUID and XMCD results are presented and discussed in Sec. III, and finally summarized in Sec. IV.

II. SAMPLE PREPARATION AND EXPERIMENTAL DETAILS

The $\text{Sm}_{1-x}\text{Gd}_x\text{Al}_2$ ($x=2.8\%$)/ SmAl_2 bilayer with [111] as the growth direction was epitaxially grown by molecular-beam epitaxy at 450 °C and for base pressures around 10^{-10} Torr. A 50 nm Nb buffer layer was first deposited on the (11 $\bar{2}$ 0) Al_2O_3 substrate in order to allow for the epitaxial growth of SGA as the bottom layer and then SA as the top layer.²⁵ Before film deposition, the Sm, Al and Gd evaporation rates were carefully calibrated in order to get the desired stoichiometry. Both layers' thicknesses were 300 nm. Simultaneously to the SGA/SA growth, part of the 300-nm-thick SGA bottom layer was kept uncovered so that the behavior of the same single SGA layer can be compared to that of the bilayer. The films were covered with 50 nm Nb as a protection against oxidation. The crystalline quality was checked

during growth by *in situ* reflection high energy electron diffraction (RHEED) and after growth by *ex situ* x-ray diffraction (XRD). RHEED patterns, formed by thin and contrasted streaks, attest for flat surfaces and the high crystalline quality of the films. XRD spectra for the bilayer and single layer show the (111) diffraction peaks of the expected Laves phase structure with a mosaicity of 0.4° and the absence of secondary phases.

High sensitivity SQUID magnetometry (maximum applied field of ± 70 kOe) was used to measure the sample net magnetization. SGA and SA epitaxial films with [111] growth direction exhibit a strong uniaxial perpendicular anisotropy attributed to magnetoelastic effects.²⁸ The results presented in this paper were thus obtained by applying the external magnetic field along the easy magnetization axis, i.e., perpendicular to the film plane.

XMCD experiments were performed on beamline ID12 at the European Synchrotron Radiation Facilities (ESRF) in a temperature range between 10 and 300 K. A magnetic field of maximum 60 kOe was applied perpendicular to the film surface and parallel to the direction of the incident x-ray beam. The XMCD spectra were recorded by flipping the helicity of incoming x-rays and keeping the direction of the magnetic field fixed. Experiments were performed for incident photon energy fixed at the Sm and Gd L edges; the second harmonic of the HELIOS-II undulator was used and the helicity of incoming photons was changed after each consecutive scan. The degree of circular polarization of the monochromatic x-ray beam was estimated to be in excess of 85%. The spectra were recorded in the total fluorescence detection mode, which is not sensitive to the external applied magnetic field, at least in the range of interest (+60 to -60 kOe).

Typical XMCD spectra at the Sm L_2 and Gd L_3 edges are shown in Fig. 1, together with the corresponding normalized x-ray absorption spectra (x-ray absorption near edge-structure curves). The XMCD is defined as the difference between the absorption for the circular polarization parallel and antiparallel to the direction of magnetization. One can underline the reasonable quality of the signal recorded at the Gd edge despite the small quantity of Gd in the system. Note however that the close proximity of a much stronger signal due to Sm affects the shape of the absorption curves. Those spectra in Fig. 1 have been recorded for the SGA/SA bilayer at 64 K for a -60 kOe applied field (H_{ext}), after a field cooling process from 150 K under +60 kOe (H_{fc}). This temperature of 64 K corresponds to the SGA compensation temperature, as it will be shown in the following.

Measurements at the L edges of rare-earth probe the transition from $2p$ core levels to $5d$ empty states; they permit to determine the projection of $5d$ spin momentum along the quantification axis, i.e., either parallel or antiparallel to the direction of applied magnetic field. Due to the so-called breathing effect, a negative (positive) signal measured at the L_2 (L_3) edge results from a positive projection of $5d$ spin polarization along the quantification axis (i.e., parallel to the positive field direction).²⁹

In the case presented in Fig. 1, the opposite signs for the signals measured at the Sm L_2 and Gd L_3 edges confirm the parallel alignment of Sm and Gd $5d$ spin momentum (see

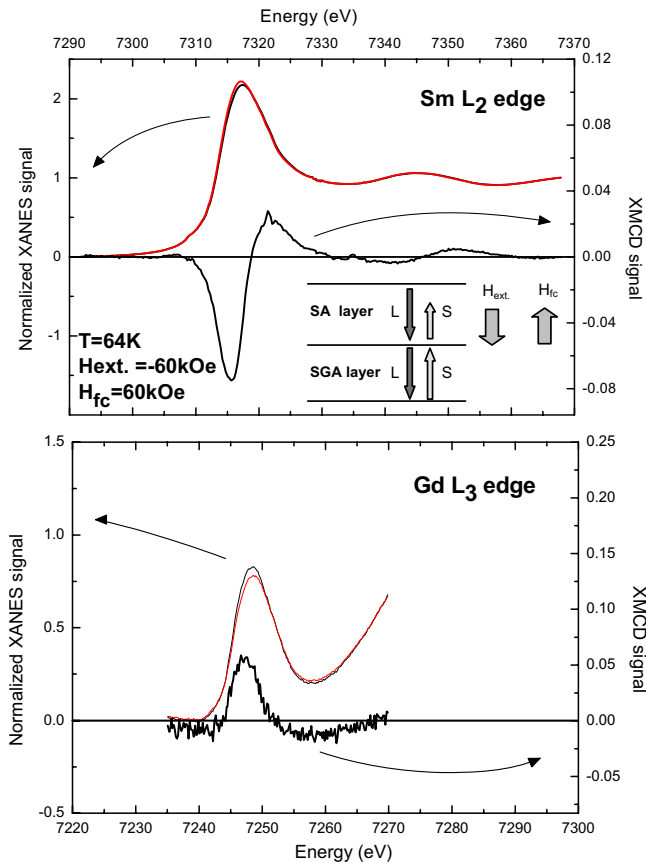


FIG. 1. (Color online) Normalized x-ray absorption near edge-structure curves and normalized x-ray magnetic circular dichroism signals recorded at the Sm L_2 (top) and Gd L_3 (bottom) edges for the $\text{Sm}_{0.972}\text{Gd}_{0.028}\text{Al}_2/\text{SmAl}_2$ bilayer. Measurements were performed at 64 K for an applied field $H_{\text{ext}} = -60$ kOe and after field cooling the system from 150 K in $+60$ kOe. The inset is a schematic view of the magnetic configurations in the SA/SGA bilayer, as deduced from the signs of Sm L_2 and Gd L_3 XMCD signals.

sketch in Fig. 1). In these specific conditions, the projections of $5d$ spin momentum are positive, thus parallel to the direction of the cooling field (H_{fc}) and antiparallel to the direction of the field applied for the measurements (H_{ext}). This configuration can be easily explained: the SGA layer is in the magnetic compensated state ($M=0$), thus the external field has no effect on the SGA orientation that is given by the cooling conditions (the S moments, dominant above T_{comp} , align parallel to the cooling field). On the contrary, the SA net magnetization orientates along the applied field: the L contribution being dominant, the S moments are opposite to the applied field.

It was verified that the shapes of the XMCD spectra do not change with field and that they exhibit a maximum for the same energy value. To record element-selective hysteresis loops, the energy of the incident x-ray photons was thus tuned to the maximum of the XMCD signal either at the Sm L_2 edge (7.316 keV) or at the Gd L_3 edge (7.247 keV). The amplitude of the dichroic signal at each value of the applied field was measured by flipping the helicity of the x-ray beam.

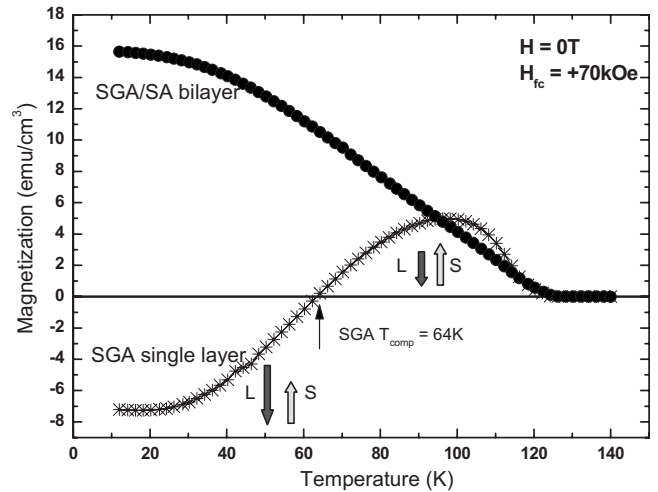


FIG. 2. Temperature-dependent magnetization curves measured while heating the sample in zero applied field, after a $+70$ kOe field cooling process, for the $\text{Sm}_{0.972}\text{Gd}_{0.028}\text{Al}_2/\text{SmAl}_2$ bilayer (filled circles) and the single $\text{Sm}_{0.972}\text{Gd}_{0.028}\text{Al}_2$ layer (crosses).

III. RESULTS AND DISCUSSION

Temperature-dependent magnetization curves were measured by SQUID for the SGA/SA bilayer and separately for the SGA single layer (Fig. 2). The results have been obtained in increasing temperature for zero applied field after cooling down the samples from room temperature under $+70$ kOe. The Curie temperature is approximately 126 K for both samples, in good agreement with results reported for bulk SmAl_2 compound.²³ The magnetization curve of the SGA/SA bilayer is the sum of the behaviors in both components and does not permit to distinguish between SA and SGA. The SGA single layer exhibits a compensated magnetic state at 64 K (T_{comp}). Its net magnetization is negative below T_{comp} and positive above T_{comp} , revealing that the L contribution (dominant below T_{comp}) is opposite to the cooling field direction and the S contribution is orientated along the cooling field direction (see sketches on Fig. 2). The measurements being performed for $H_{\text{ext}}=0$, the magnetic configuration namely remains the one stabilized while cooling the film: the S contribution, dominant at high temperature, aligns with the cooling field. This configuration persists down to low temperature despite the change in dominant contribution because the coercive field is then likely too high for the magnetization to reverse.

The interface exchange coupling and the resulting exchange-bias field in the bilayer system have been explored by the measurement of hysteresis loops after field cooling in $+60$ kOe from 150 K. Figure 3 presents typical hysteresis loops measured for the SGA/SA bilayer, at 20 and 64 K. Those measured for the SGA single layer are shown in inset. The loops recorded for the bilayer at these temperatures exhibit a unique step. This is attributed to the reversal of the SA magnetization since the SGA magnetization, measured in the single layer, does not vary with field in this temperature range (see inset). The loops are shifted horizontally toward positive fields by a bias field H_{B} and vertically by a quantity called ΔM .

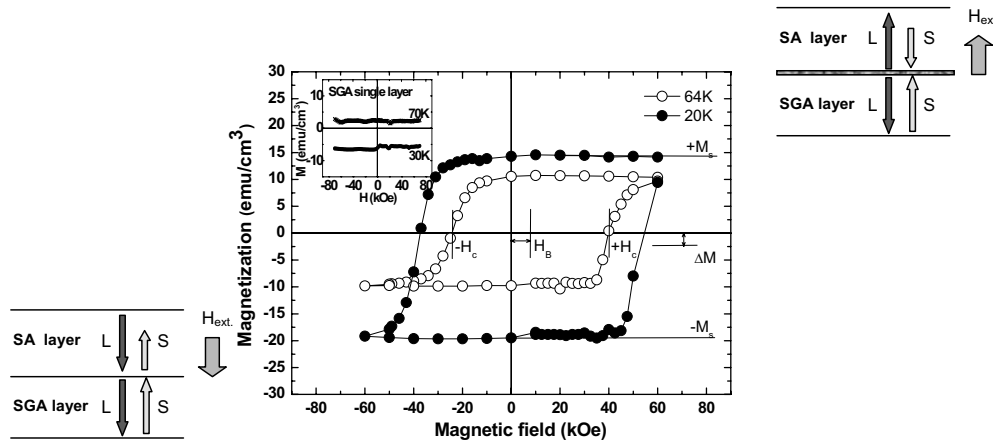


FIG. 3. Magnetization measurements of the $\text{Sm}_{0.972}\text{Gd}_{0.028}\text{Al}_2/\text{SmAl}_2$ bilayer performed at 20 K (filled circles) and 64 K (empty circles) with the magnetic field applied perpendicular to the sample surface (prior to measurements, the system has been field cooled from 150 K in 60 kOe). The inset corresponds to similar measurements performed on the single SGA layer at 70 and 30 K. The sketches present the magnetic configurations expected for large positive (top right) and large negative (bottom left) magnetic fields.

The positive horizontal shift proves a strong exchange coupling between the SA and SGA layers and can be accounted for by assuming the magnetic configurations sketched for large positive and negative fields in Fig. 3. After the field-cooling process, the SGA spin contribution is oriented along the positive H_{fc} , as it has been deduced from the temperature dependence (Fig. 2), and remains in this orientation in the available field range. Concerning the SA layer, its magnetization is dominated by the L contribution which thus aligns with H_{ext} for large positive and negative fields. For large positive fields, the L (and S) contributions in the SA and SGA layers are thus pointing in opposite directions, which results in a high energy interface because of the frustrated exchange coupling. This tends to favor the SA magnetization reversal and gives rise to a *positive* exchange bias. One can notice that the exchange-bias effect is also present at 64 K, in agreement with the persisting exchange coupling between SGA and SA despite the SGA zero magnetization state. The value of exchange-bias field can be used to estimate the interfacial exchange energy $\sigma = H_{EB} 2M_{SA}t_{SA}$, where M_{SA} and t_{SA} are the magnetization and thickness of the SA layer. At 20 K, considering the magnetic reversal of 300 nm SA with a magnetization density of 30 emu/cm^3 , this gives an interfacial exchange energy close to 12.5 erg/cm^2 at 20 K, i.e., one or two orders of magnitude higher than in the AFM/FM systems. This can be attributed to the coupling occurring between all spin moments while it is limited to uncompensated moments in AFM-based systems. The temperature dependence of the bias field measured after the +60 kOe field cooling is presented Fig. 4(b) (filled circles). It exhibits an unusual nonmonotonous behavior that will be discussed later in the paper.

The vertical shift ΔM is signature of pinned magnetization in the system and likely is a consequence of the nonreversal of the SGA layer. ΔM is negative below T_{comp} , where the SGA net magnetization is negative. Measurements performed above T_{comp} , where the SGA net magnetization becomes positive exhibit a positive vertical shift. One can also notice that the vertical shift is *zero* at 64 K, in agreement

with the vanishing SGA magnetization. In Fig. 4(a), the temperature dependence of ΔM (filled squares) has been superimposed on the magnetization curve measured for the single SGA layer (crosses) to allow for a better comparison. The agreement is satisfactory between approximately 60 and 80 K, but outside this range, ΔM is significantly smaller than what is expected from the totally pinned SGA single layer. Above 80 K, measurements performed for the SGA single layer attest for a partial magnetization reversal in this field range, which likely also occurs in the bilayer system. However, below 60 K, the SGA magnetization in the single layer does not change with field in the field range available with the SQUID magnetometer. The difference at low temperature between ΔM and the single-layer magnetization can have two origins: (i) the SGA layer in SGA/SA is fully pinned, as in the single layer, but its net magnetization is reduced compared to the single SGA layer, because of the presence of domains and/or regions of nonhomogeneous magnetization. (ii) Part of the SGA layer is driven to reverse by interface exchange coupling to the SA layer.

SQUID magnetometry does not permit us to discriminate between these hypotheses since the technique averages over both SA and SGA magnetization. The vanishing magnetization of SGA around T_{comp} also prevents from any analysis in the zero-magnetization state.

To address this issue in further details, the element selectivity provided by XMCD enables to probe the bottom SGA layer separately, for incident photon energy tuned to a Gd absorption edge. Its sensitivity to the *spin polarization* also permits to probe the SGA at T_{comp} , and consequently to investigate how the SA reversal may influence the zero-magnetization configuration. Figure 5 gathers the XMCD hysteresis loops measured at 20 K (filled symbols) and 64 K (empty symbols), for incident photons energy tuned to the Sm L_2 (top curves) and Gd L_3 (bottom curves) edges. The loops measured at the Sm edge reflect the behavior of the whole system, as those recorded by SQUID magnetometry while those recorded at the Gd edge specifically probe the bottom SGA layer. In relatively good agreement with SQUID

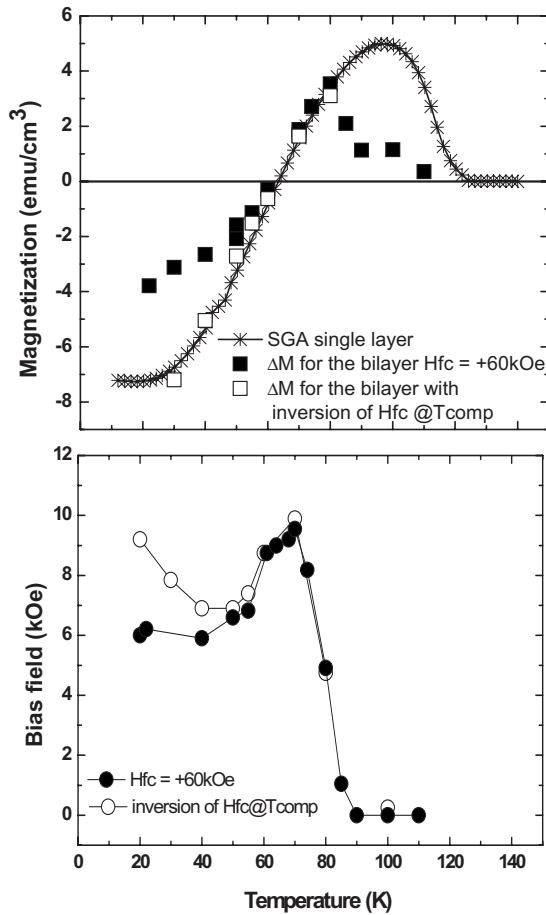


FIG. 4. (a) Temperature dependence of the vertical shift (ΔM) of the hysteresis loops recorded for the $\text{Sm}_{0.972}\text{Gd}_{0.028}\text{Al}_2/\text{SmAl}_2$ bilayer, superimposed to the temperature dependence of the single $\text{Sm}_{0.972}\text{Gd}_{0.028}\text{Al}_2$ layer magnetization (crosses). Hysteresis loops have been measured after field cooling under +60 kOe (filled squares) and with inversion of the cooling field at T_{comp} (empty squares). (b) Temperature dependence of the exchange-bias field deduced from the $\text{Sm}_{0.972}\text{Gd}_{0.028}\text{Al}_2/\text{SmAl}_2$ bilayer hysteresis loops, after field-cooling under +60 kOe (filled circles) and with inversion of the cooling field at T_{comp} (empty circles).

results, the loops recorded at the Sm edge exhibit positive horizontal shifts at 20 and 64 K. The loops are also vertically shifted toward the negative values. The asymmetry of the XMCD loops respect to the x-axis is however much stronger than for SQUID loops; the XMCD vertical shift is namely due to *pinned spin polarization* during the reversal process, and not to *pinned magnetization*. It is especially obvious that the XMCD loop measured at T_{comp} is still shifted while the SQUID loop measured at the same temperature is symmetrical respect to the x axis. At T_{comp} , the pinned moments in SGA do not contribute to magnetometry results but the pinned *spin contribution* still largely contributes to XMCD measurements.

XMCD loops recorded at the Gd edge show that the SGA behavior in the SA/SGA bilayer is completely different from the one recorded in the single SGA layer. In this latter, the XMCD signal does not change with field in the -60 kOe/+60 kOe range (see inset in Fig. 5). In the bilayer, the bot-

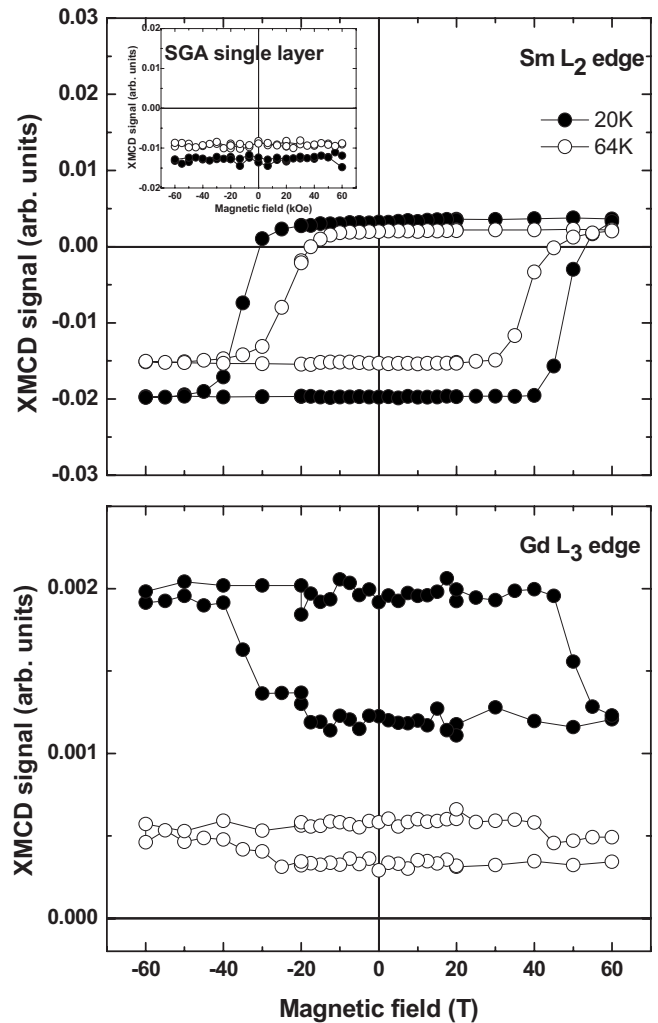


FIG. 5. Element-selective hysteresis loops measured by XMCD for the $\text{Sm}_{0.972}\text{Gd}_{0.028}\text{Al}_2/\text{SmAl}_2$ bilayer at 20 K (filled circles) and 64 K (empty circles), for incident photons energy tuned to the Sm L_2 edge (top curves) and Gd L_3 (bottom curves) absorption edges. Prior each measurement, the system has been field cooled from 150 K in +60 kOe. The inset in the top part corresponds to XMCD measurements performed at the Sm L_2 edge for the same temperatures and in same conditions for the $\text{Sm}_{0.972}\text{Gd}_{0.028}\text{Al}_2$ uncovered single layer.

tom SGA layer exhibits partial magnetization reversal, even at 64 K where its zero magnetization does not interact with the external field. Those Gd loops are vertically shifted, which means that part of the SGA moments are pinned while others rotate with the external field. The ratio between the pinned and rotatable moments can be determined from the ratio between the loop vertical shift and half the loop amplitude. It appears that approximately 20% of the SGA moments rotate with the external field while the remaining 80% are pinned. The coercive fields related to this SGA partial reversal have been determined as the field for which the XMCD signal is average of the maximum and minimum values. At 20 K, those are -35 and 49 kOe, in perfect agreement with the reversal recorded at the Sm edge. At 64 K, the coercive fields at the Gd edge are relatively similar to those measured at 20 K (-38 and 45 kOe) while the values re-

corded at the Sm edge are smaller, by approximately 10 kOe. These results suggest that the partial SGA reversal is driven by exchange coupling at the interface with SA. Because of the poorer signal/background ratio at the Gd edge and at 64 K, it is difficult to determine whether the discrepancy between Sm and Gd coercive fields at this temperature is relevant. This could result from a delayed SGA reversal compared to the SA one, especially at this temperature where the Zeeman energy does not contribute to the SGA reversal but complementary experiments are necessary to confirm such a feature.

Let us now discuss the proportion of rotatable SGA moments. Given the SGA layer thickness, 20% of rotatable moments correspond to an effective thickness of 60 nm. A similar analysis performed for the XMCD loops recorded at the Sm edge reveals that 60% of the Sm polarization rotates with the field, which, given the total thickness of the bilayer, corresponds to an effective thickness of 360 nm. Those results are both consistent with the complete reversal of the SA layer (300 nm thick) and the reversal of 60 nm of the SGA layer. Given the schematic illustration of magnetic configurations for large positive and negative fields (see sketches in Fig. 3), the partial reversal of the SGA layer may correspond to the moments involved in the interface domain wall (iDW) present for positive fields. In that case, because the iDW yields no net polarization along the positive applied field, a 120-nm-thick iDW is required to account for the amplitude of the Gd polarization loop (effective thickness of 60 nm).

This value is much larger than the domain wall thickness expected in such compounds: given an exchange constant around $0.5 \cdot 10^{-7}$ erg/cm³⁰ and an anisotropy constant close to 1.10^{-7} erg/cm³,³¹ the calculated domain-wall thickness under zero field is only 3.6 nm, and is approximately unchanged under 60 kOe because of the very small magnetization density in this SGA compound (7 emu/cm³ at 20 K). In the hypothesis of a 120 nm thick uniform iDW in SGA, one can determine an effective anisotropy constant, and calculate the resulting exchange-bias field ($H_{EB} = 4\sqrt{A_{SGA}K_{SGA}/2M_{SA}t_{SA}}$). This yields a bias field of 78 Oe, i.e., two orders of magnitude smaller than the one measured at 20 K (7000 Oe).

Those discrepancies make us consider another scenario that could account for the experimental observations. A possible alternative to the uniform iDW is the presence of lateral domains in the SGA layer for positive applied fields (parallel to the cooling field) as it is sketched in Fig. 6. The P domains (SA and SGA magnetic contributions parallel to each other) correspond to the configuration expected at low temperature from both Zeeman and exchange contributions. The AP domains (SA and SGA moments antiparallel to each other) correspond to the configuration expected if the positive cooling field is not strong enough to reverse the SGA moments below T_{comp} . AP domains thus result from the strong coercivity in SGA, while P domains develop below T_{comp} most likely in area of locally lower coercivity, where exchange coupling to SA and interactions with the applied field enable the SGA reversal. At the compensation temperature, P domains are not favored by the positive cooling field but might result from exchange with the SA layer. In this hypothesis, AP domains in SGA constitute the pinned part of the SGA layer because

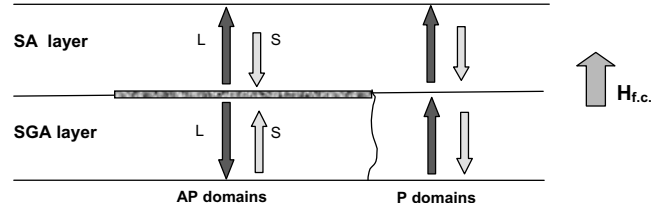


FIG. 6. Schematic view of the possible magnetic configuration in the $\text{Sm}_{0.972}\text{Gd}_{0.028}\text{Al}_2/\text{SmAl}_2$ bilayer, below T_{comp} , for positive applied fields (parallel to the cooling field), in the case of coexisting domains in the bottom SGA layer.

their orientation is favored by exchange and Zeeman contributions for negative applied fields. The rotatable part of the SGA layer most likely corresponds to P domains, although some of the P domains might also be pinned.

For relatively small domains in SGA, the reversal of the SA layer will average the underlying SGA configuration.^{6,32} The exchange bias field is thus expected to depend of course on the domain wall energy in these compounds but also on the relative proportions of AP and P domains in SGA and on the ability of those P domains to rotate: $H_{EB} = +x\sigma/2M_{SA}t_{SA} - (1-y)(1-x)\sigma/2M_{SA}t_{SA}$ with x the proportion of AP domains and y the proportion of rotatable domains respect to the $(1-x)$ P domains. Only pinned domains of course contribute to the bias field. x AP domains yield positive exchange bias, while $(1-y)(1-x)$ P domains lead to negative exchange bias. Rotatable SGA [$y(1-x)$] leads to zero bias field. Both the relative proportions of P and AP domains and the proportion of pinned P domains can give rise to the unusual non monotonous dependence of bias field upon temperature, with a pronounced increase around the SGA compensation temperature [Fig. 4(b)]. From the expression given above an increase (decrease) in x and y drives the increase (decrease) in exchange-bias field. In the temperature range close to compensation, the SGA magnetization vanishes and the Zeeman contribution does not help in forming P domains; the relative proportion of AP domains (x) is likely larger than at lower temperature. Since the proportion of rotatable SGA [$y(1-x)$] is approximately the same at 20 K and at 64 K (around 20% from XMCD results), the increase in x is most likely accompanied by an increase in y , both contributing to the increase of the bias field.

In order to confirm the presence of SGA domains and their role on exchange bias, a particular cooling process has been used to prevent from their formation during cooling. The sample is field cooled in +70 kOe from 150 K down to T_{comp} (the dominant S contribution aligns along the positive cooling field) and then in -70 kOe from T_{comp} down to the measurement temperature (the negative cooling field then points toward the dominant L contribution). With this cooling procedure, the SGA magnetic configuration with S pointing toward the positive field direction and L pointing opposite (AP arrangement respect to the SA layer) should be stabilized over the entire temperature range: no lateral domains are thus expected to form in the SGA layer. This is supposed to be drastically different from the configuration stabilized by the usual cooling procedure under positive field: in this case, at some temperature below T_{comp} , the *posi-*

tive cooling field namely drives the magnetization flip in some domains to align dominant L moments parallel to H_{fc} . Coexisting AP and P domains are thus formed in the SGA layer.

The magnetization shifts and exchange-bias fields measured after the cooling procedure with reversal of H_{fc} at T_{comp} are reported in Fig. 4 (empty squares and empty circles). The vertical magnetization shift ΔM now perfectly matches the SGA single layer magnetization, in agreement with a pinned SGA layer with no lateral domains in the bilayer. Simultaneously, the bias field obtained *below* 50 K is significantly increased, consistently with a larger amount of pinned SGA contributions at the interface. The difference in bias field measured at 20 K after the two different cooling is approximately 33%. This value is larger than the 20% rotatable contribution determined from XMCD experiments after the +60 kOe cooling process. This discrepancy suggests that non rotatable P domains also contribute (negatively) to the bias field measured after the +60 kOe cooling. *Above* 50 K, the bias fields measured after the two cooling procedures are very similar with a pronounced increase in temperature around the SGA magnetic compensation. Close to T_{comp} , the temperature dependence of exchange bias obviously results from a delicate balance between the intrinsic variation in exchange bias upon temperature and the proportion of AP and P domains. P domains may still develop *after the cooling process*, when applying the large initial positive field at the beginning of the loop.

IV. CONCLUSION

In conclusion, $\text{Sm}_{1-x}\text{Gd}_x\text{Al}_2/\text{SmAl}_2$ bilayer is an original exchange-coupled system combining a ferromagnet domi-

nated by orbital contributions (SA) and the only experimental realization of a zero-magnetization ferromagnet (SGA). When field cooled under +60 kOe, the system exhibits a strong positive exchange-bias effect, attributed to the positive exchange coupling between spin contributions in both compounds, and to the orientation of the pinned SGA moments. The amount of pinned magnetization however does not reach the value expected from a homogeneously magnetized pinned SGA layer. XMCD experiments have permitted to clarify this issue. Measurements have been performed at the Gd absorption edge to probe the SGA behavior, both out of and in the magnetic compensated state. It appears that, in the temperature range investigated, 20% of the SGA layer is driven to reverse under field. This reversal is achieved via exchange coupling at the interface, as proved by the observation of a partial SGA reversal even at the compensation temperature where its magnetization drops to zero and thus does not interact with the external field. The large amount of rotatable SGA moments in comparison with the domain wall thickness expected in such compounds suggests the coexistence of domains with opposite orientations in the SGA layer; those will constitute pinned and rotatable components. The temperature dependence of the ratio between pinned and rotatable domains could account for the nonhomogeneous variation in exchange-bias field upon temperature measured by SQUID magnetometry.

ACKNOWLEDGMENTS

We are grateful to Danielle Pierre for her help with the sample preparation.

-
- ¹M. Sawicki, G. J. Bowden, P. A. J. de Groot, B. D. Rainford, J. M. L. Beaujour, R. C. C. Ward, and M. R. Wells, *Appl. Phys. Lett.* **77**, 573 (2000).
- ²K. Dumesnil, S. Fernandez, A. Avisou, C. Dufour, A. Rogalev, F. Wilhelm, and E. Snoeck, *Eur. Phys. J. B* **72**, 159 (2009).
- ³A. E. Berkowitz and K. Takano, *J. Magn. Magn. Mater.* **200**, 552 (1999).
- ⁴J. Nogués and I. K. Sculler, *J. Magn. Magn. Mater.* **192**, 203 (1999).
- ⁵B. Dieny, V. S. Speriosu, S. S. P. Parkin, B. A. Gurney, D. R. Wilhoit, and D. Mauri, *Phys. Rev. B* **43**, 1297 (1991).
- ⁶K. Dumesnil, C. Dufour, S. Fernandez, M. Oudich, A. Avisou, A. Rogalev, and F. Wilhelm, *J. Phys.: Condens. Matter* **21**, 236002 (2009).
- ⁷S. Mangin, G. Marchal, and B. Barbara, *Phys. Rev. Lett.* **82**, 4336 (1999).
- ⁸C.-C. Lin, C.-H. Lai, R.-F. Jiang, and H.-P. D. Shieh, *J. Appl. Phys.* **93**, 6832 (2003).
- ⁹E. E. Fullerton, J. S. Jiang, M. Grimsditch, C. H. Sowers, and S. D. Bader, *Phys. Rev. B* **58**, 12193 (1998).
- ¹⁰X. H. Chen, K. Q. Wang, P. H. Hor, Y. Y. Xue, and C. W. Chu, *Phys. Rev. B* **72**, 054436 (2005).
- ¹¹P. D. Kulkarni, A. Thamizhavel, V. C. Rakhecha, A. K. Nigam, P. L. Paulose, S. Ramakrishnan, and A. K. Grover, *EPL* **86**, 47003 (2009).
- ¹²A. P. Malozemoff, *Phys. Rev. B* **35**, 3679 (1987).
- ¹³D. Mauri, H. C. Siegmann, P. S. Bagus, and E. Kay, *J. Appl. Phys.* **62**, 3047 (1987).
- ¹⁴M. Gruyters and D. Schmitz, *Phys. Rev. Lett.* **100**, 077205 (2008).
- ¹⁵S. Brück, G. Schütz, E. Goering, X. Ji, and K. M. Krishnan, *Phys. Rev. Lett.* **101**, 126402 (2008).
- ¹⁶H. Ohldag, H. Shi, E. Arenholz, J. Stöhr, and D. Lederman, *Phys. Rev. Lett.* **96**, 027203 (2006).
- ¹⁷M. R. Fitzsimmons, B. J. Kirby, S. Roy, Z.-P. Li, I. V. Roshchin, S. K. Sinha, and I. K. Schuller, *Phys. Rev. B* **75**, 214412 (2007).
- ¹⁸S. Roy, M. R. Fitzsimmons, S. Park, M. Dorn, O. Petravic, I. V. Roshchin, Z.-P. Li, X. Battle, R. Morales, A. Misra, X. Zhang, K. Chesnel, J. B. Kortright, S. K. Sinha, and I. K. Schuller, *Phys. Rev. Lett.* **95**, 047201 (2005).
- ¹⁹A. Hoffmann, J. W. Seo, M. R. Fitzsimmons, H. Siegwart, J. Fompeyrine, J. P. Locquet, J. A. Dura, and C. F. Majkrzak, *Phys. Rev. B* **66**, 220406(R) (2002).
- ²⁰H. Adachi and H. Ino, *Nature (London)* **401**, 148 (1999).
- ²¹H. Adachi, H. Ino, and H. Miwa, *Phys. Rev. B* **59**, 11445 (1999).
- ²²J. W. Taylor, J. A. Duffy, A. M. Bebb, M. R. Lees, L. Bouchenoire, S. D. Brown, and M. J. Cooper, *Phys. Rev. B* **66**, 161319 (2002).

- ²³H. Adachi, H. Kawata, H. Hashimoto, Y. Sato, I. Matsumoto, and Y. Tanaka, *Phys. Rev. Lett.* **87**, 127202 (2001).
- ²⁴S. Qiao, A. Kimura, H. Adachi, K. Iori, K. Miyamoto, T. Xie, H. Namatame, M. Taniguchi, A. Tanaka, T. Muro, S. Imada, and S. Suga, *Phys. Rev. B* **70**, 134418 (2004).
- ²⁵A. Avisou, C. Dufour, K. Dumesnil, and D. Pierre, *J. Cryst. Growth* **297**, 239 (2006).
- ²⁶A. Avisou, K. Dumesnil, and C. Dufour, *J. Magn. Magn. Mater.* **316**, 317 (2007).
- ²⁷A. Avisou, C. Dufour, K. Dumesnil, A. Rogalev, F. Wilhelm, and E. Snoeck, *J. Phys.: Condens. Matter* **20**, 265001 (2008).
- ²⁸A. Avisou, C. Dufour, and K. Dumesnil, *J. Appl. Phys.* **103**, 07E135 (2008).
- ²⁹J. C. Parlebas, K. Asakura, A. Fujiwara, I. Harada, and A. Kotani, *Phys. Rep.* **431**, 1 (2006).
- ³⁰A. Barla, J. P. Sanchez, F. Givord, J. X. Boucherle, B. P. Doyle, and R. Ruffer, *Phys. Rev. B* **71**, 012407 (2005).
- ³¹A. Avisou, Ph.D. thesis, Université H. Poincaré Nancy I, 2006.
- ³²I. V. Roshchin, O. Petracic, R. Morales, Z. P. Li, X. Battle, and I. K. Schuller, *Europhys. Lett.* **71**, 297 (2005).